RERG suppresses cell proliferation, migration and angiogenesis through ERK/NF-κB signaling pathway in nasopharyngeal carcinoma

Weilin Zhao[1,2,3], Ning Ma[4], Shumin Wang[1,3,5] , Yingxi Mo[1,3,6], Zhe Zhang[3], Guangwu Huang[3], Kaoru Midorikawa[1], Yusuke Hiraku[1], Shinji Oikawa[1], Mariko Murata[1,*], Kazuhiko Takeuchi[2,*]

[1]Department of Environmental and Molecular Medicine, Mie University Graduate School of Medicine, Tsu, Mie, Japan, [2]Department of Otorhinolaryngology - Head and Neck Surgery, Mie University Graduate School of Medicine, Tsu, Mie, Japan, [3]Department of Otolaryngology Head and Neck Surgery, First Affiliated Hospital of Guangxi Medical University, Nanning, Guangxi, China, [4]Graduate School of Health Science, Suzuka University of Medical Science, Suzuka, Mie, Japan

[*]Corresponding authors.

Professor Mariko Murata, Department of Environmental and Molecular Medicine, Mie University Graduate School of Medicine, 2-174, Edobashi, Tsu, Mie, 514-8507, Japan.

Tel.: +81 59 231 5011, Fax: +81 59 231 5011. E-mail address: mmurata@doc.medic.mie-u.ac.jp

Professor Kazuhiko Takeuchi, Department of Otorhinolaryngology - Head and Neck Surgery, Mie University Graduate School of Medicine, 2-174, Edobashi, Tsu, Mie, 514-8507, Japan,

Tel.: +81 59 231 5028, Fax: +81 59 232 9582.

E-mail address: kazuhiko@clin.medic.mie-u.ac.jp

[5]Present address: Center for Oral Biology, University of Rochester Medical Center, Rochester, NY, USA

[6]Present address: Department of Research, Affiliated Tumor Hospital of Guangxi Medical University, Nanning, Guangxi, China

Key words: *RERG*; Nasopharyngeal carcinoma; Tumor suppressor gene; DNA methylation; Angiogenesis.

Abbreviations: AUC, Area under the curve; Aza, 5-Aza-2'-deoxycytidine; BGS, Bisulfite genomic sequencing; CCK8, Cell counting kit-8; DAPI, 4',6-diamidino-2-phenylindole; EBV, Epstein-Barr virus; HDAC, Histone deacetylase; IHC, Immunohistochemistry; IL6, Interleukin-6; IL8, Interleukin-8; MMPs, Matrix metalloproteinases; MTT, 3-(4,5-dimethylthiazol-2-yl)-2,5-diphenyl tetrazolium bromide; NNE, non-cancerous nasopharyngeal epithelia; NPC, Nasopharyngeal carcinoma; PCNA, Proliferating cell nuclear antigen; *RERG*, Ras- like estrogen-regulated growth inhibitor; ROC, Receiver operating characteristic; TIMPs, Tissue inhibitors of metalloproteinases; TNFα, Tumor necrosis factor-α; TSA, Trichostatin A; TSG, Tumor suppressor gene; VEGF, Vascular endothelial growth factor.

Abstract

Background: Nasopharyngeal carcinoma (NPC) is a malignancy of the head and neck that is prevalent in Southeast Asia and southern China. Recent studies in epigenetics suggest that DNA methylation plays a pivotal role in the onset and progression of cancer. Combining the methyl-DNA binding domain capture technique and cDNA microarray analysis, we identified a unique hypermethylated gene, *RERG* (Ras-like estrogen-regulated growth inhibitor), that was down-regulated in NPC tissues. *RERG* is a tumor suppressor gene that was first reported in breast cancer. However, the functions of *RERG* are largely unknown in other tumor types.

Methods: RERG expression was assessed in human subjects (NPC primary tissues and non-cancer tissues) and cell lines (NPC cell lines and an immortalized epithelial cell line NP460). Further, we investigated the methylation rate of *RERG* in both human subject and cell lines. 5-Aza-2'-deoxycytidine (Aza) or combined with trichostatin A (TSA) were treated to three NPC cell lines (HK1, C666-1 and HK1_EBV). In addition, the role of RERG in NPC cells and its underlying mechanisms were explored by overexpression of RERG in NPC cell lines.

Results: *RERG* was significantly down-regulated in NPC cancer nests compared to normal nasopharyngeal epithelium cells. Furthermore, the *RERG* promoter was frequently methylated in NPC tissues and cell lines. The *RERG* methylation rate yielded an area under the curve (AUC) of receiver operating characteristic (ROC) curve was 0.897 (95%CI: 0.818–0.976). The down-regulation of *RERG* was restored in NPC cells treated with Aza and TSA. In addition, ectopic expression of *RERG* in NPC cell lines resulted in a significant suppression of cell proliferation, clonogenicity, migration and invasion. *RERG*-overexpressing cells showed significantly slower growth and less angiogenesis in tumor xenografts in nude mice. *RERG* suppressed the

ERK/NF-κB signaling pathway and inhibited tumor growth and angiogenesis with down-regulation of MMPs and IL8 in tumors of nude mouse xenografts.

Conclusions: Our results suggest that *RERG* is frequently silenced by promoter CpG methylation in NPC, and acts as a functional tumor suppressor by suppressing the ERK/NF-κB signaling pathway. These findings support the potential use of RERG as a novel molecular target in NPC therapy.

Background

Nasopharyngeal carcinoma (NPC) is a common head and neck malignancy and important health issue in Southeast Asia and southern China although it is rare in Japan and Western countries.[1] It is closely associated with Epstein-Barr virus (EBV) [2] and shows highly invasive and metastatic features.[3] Evidence in recent years suggests that additional genetic and epigenetic abnormalities are necessary to drive the tumorigenic process. Epigenetic changes, which involve DNA methylation and histone modifications, play critical roles in the onset and progression of cancer and other diseases.[4, 5] Hypermethylation of CpG islands is a well-recognized epigenetic event in cancer.[6] Hypermethylated genomic regions frequently mediate the silencing of tumor suppressor genes (TSGs).[6, 7] Recent studies indicate that epigenetic processes occur very early in cancer development and may contribute to cancer initiation.[8] Epigenetic inactivation of potential TSGs by aberrant promoter DNA methylation has been increasingly recognized to play a key role in the tumorigenesis of NPC by altering gene functions during cell proliferation, apoptosis, and differentiation.[2, 7, 9] The discovery of epigenetic changes may prove to be extremely useful for early detection and prevention of cancer, including NPC.[10, 11]

Ras-like estrogen-regulated growth inhibitor (*RERG*) was initially identified as a candidate tumor suppressor gene, and is regulated by estrogen in breast tumors.[12, 13] *RERG* is located on chromosome 12p12 and encodes a small GTP-binding and hydrolyzing protein (GTPase) of the Ras superfamily. *RERG* is widely expressed in multiple normal tissues, while *RERG* expression is lost in breast, kidney, ovary, and colon tumor tissues.[12, 14] It has been reported that *RERG* is a prognostic marker in breast cancer, and its expression has correlated

inversely with proliferation, patient survival, and the development of distant metastases.[15] Significantly hypermethylated *RERG* was also observed in colorectal adenocarcinoma,[16, 17] and breast cancer.[18] These findings suggest that *RERG* acts as a putative TSG, but the functions of *RERG* in NPC have yet to be identified.

Recent studies indicated that multiple signaling pathways, including mitogen-activated protein kinases (MAPKs), NF-κB, Wnt/β-catenin, EGFR signaling are involved in several human cancers.[19-22] The ERK and NF-κB signaling pathway are known to promote tumor progression and angiogenesis.[23-25] It has been reported that *RERG* was involved in Ras/MEK/ERK signaling pathway in breast cancer.[12, 18] However, the relationship between *RERG* and NF-κB in NPC is still unclear.

Our genome-wide analyses using methyl-capture sequencing and cDNA microarrays have indicated that *RERG* is a candidate TSG in NPC. In the present study, we investigated the epigenetic regulation and potential tumor suppressor function of *RERG* in NPC. *RERG* was found to be epigenetically inactivated in NPC, and ectopic expression of *RERG* reduced cell proliferation, clonogenicity, migration and invasion. In addition, *RERG* suppressed angiogenesis, functioning as a repressor of ERK/NF-κB activation and inhibiting the expression of matrix metalloproteinases (MMPs), interleukin 8 (IL8) and interleukin 6 (IL6) in NPC cells. Overall our data demonstrate that *RERG* acted as a functional TSG by deactivating ERK/NF-κB signaling effectors, and *RERG* is frequently silenced in NPC.

Methods

NPC primary tumor biopsies and non-cancerous nasopharyngeal epithelia (NNE)

This study was performed with ethical review committee approval (2009–07–07) from

the First Affiliated Hospital of Guangxi Medical University, China, and ethical approval (No. 1116) from Mie University, Japan. As shown in Table 1, primary NPC tumor biopsies were obtained from 52 newly diagnosed and untreated cases (39 males and 13 females, 44.5 ± 13.9 y.o.). The diagnoses were made by experienced pathologists according to the World Health Organization (WHO) classification, and revealed that 98.1% of cases were non-keratinizing carcinoma. A total of 17 NNE samples obtained by tonsillectomy were used as controls (11 males and 6 females, 40.1 ± 14.9 y.o.). Biopsy samples were stored in a freezer at –80 °C. Biopsies of 13 untreated primary NPC tumors (7 males and 6 females, 39.5 ± 7.9 y.o.) and 9 from NNE subjects (4 males and 5 females, 52.2 ± 13.4 y.o.) were obtained for immunohistochemistry (IHC) staining, and all NPC cases were non-keratinizing carcinoma.

Cell lines

A series of NPC cell lines (HK1, C666-1, HK1_EBV) and the immortalized epithelial cell line NP460 were a kind gift from Professor Sai-Wah Tsao (Hong Kong University).[2, 26-28] Cells were maintained at 37°C in a 5% CO_2 incubator. NPC cells were cultured in RPMI1640 medium (Gibco, Grand Island, NY, USA) supplemented with 10% fetal bovine serum (FBS, Gibco), 100 U/mL penicillin, and 0.1 mg/mL streptomycin. Cells from the immortalized nasopharyngeal epithelial cell line NP460 were maintained in a 1:1 ratio of Defined Keratinocyte-SFM (Gibco) supplemented with growth factors and Epilife medium supplemented with Epilife defined growth supplement (Gibco), 100 U/mL penicillin, and 100 μg/mL streptomycin.

RNA extraction and quantitative RT-PCR

Total RNA from the biopsy samples and cell lines was isolated with TRIzol reagent

(Invitrogen, Carlsbad, CA, USA). Reverse transcription was performed using the miScript II RT kit (Qiagen, Hilden, Germany). Quantitative RT-PCR (qRT-PCR) was performed using the miScript SYBR Green PCR kit (Qiagen) and QuantiTect Primer Assay (Qiagen) by using StepOnePlus Real-Time PCR Systems (Applied Biosystems, Waltham, MA, USA). mRNA expression levels were normalized against the corresponding levels of *GAPDH*. Relative expression levels of NPC relative to NNE were calculated using the ΔΔCt method.[29]

qPCR to quantify DNA methylation rate

Genomic DNA was extracted from cell lines and biopsy tissues using a QIAamp DNA mini kit (Qiagen). To quantify gene promoter methylation, EpiTect Methyl II PCR Assay (SA Bioscience, Qiagen, Hilden, Germany) was used according to the manufacturer's instructions. In briefly, genomic DNA was exposed to digestion performed by using EpiTect Methyl II DNA Restriction Kit (SA Bioscience, Qiagen). Four reaction digestions were labelled as: no-enzyme (*Mo*), methylation sensitive enzyme (*Ms*), methylation dependent enzyme (*Md*) and methylation sensitive and dependent enzymes (*Msd*). The reaction digestions were incubated at 37°C overnight. After incubation, the reactions were stopped by heating-inactivating the enzymes at 65°C for 20 min. Methyl qPCR was carried out for each of the four digestions (*Mo*, *Ms*, *Md* and *Msd*) using the RT^2 SYBR Green ROX qPCR Mastermix (SA Bioscience, Qiagen) and EpiTect Methyl II PCR Primer Assay (SA Bioscience, Qiagen).

DNA bisulfite treatment and promoter methylation analysis

One microgram of genomic DNA was modified by sodium bisulfite by the EpiTect Bisulfit kit (Qiagen). Bisulfite genomic sequencing (BGS) were performed as previously described.[30] BGS was carried out for 40 cycles using Platinum Taq DNA Polymerase High Fidelity (Invitrogen) with BGS primers (*RERG*-BGS-F: GGAGTTTGGAGGTTTGGAAAT

and *RERG*-BGS-R: CAAAAACAAATACCAATAACCC). Amplified BGS products were subcloned and transformed into JM109 competent *Escherichia coli* cells (Promega, Madison, WI, USA). At least 5 clones for each sample were randomly chosen for sequencing.

5-Aza-2'-deoxycytidine (Aza) and trichostatin A (TSA) treatment

NPC cells (1×10^5) were seeded into 100-mm dishes and allowed to grow overnight. The culture medium was then replaced with fresh medium containing Aza at a final concentration of 10 μmol/L (Sigma-Aldrich, St. Louis, MO, USA). Cells were allowed to grow for 72 h with the Aza-containing medium changed every 24 h, and some were further treated with the histone deacetylase (HDAC) inhibitor TSA (Sigma-Aldrich) for an additional 24 h. Cells were then harvested for RNA and DNA extraction.

Vector construction and transfection

The full-length open reading frame (ORF) of *RERG* (NM_032918) was cloned into pCMV6-Entry (Origene, Rockville, MD, USA) with SgfI and MluI to generate pCMV6-*RERG*, which carries a flag tag in the N-terminal of *RERG*. Amplified ORF products with ORF primers (*RERG*-CDS-F: GAGGCGATCGCCATGGCTAAAAGTGCGGAG and *RERG*-CDS-R: GCGACGCGTACTACTGATTTTGGTGAGCAT) were subcloned and transformed into JM109 competent *Escherichia coli* cells (Promega, Madison, WI, USA). Construction of recombinant pCMV6-*RERG* was validated by sequencing.

Three NPC cell lines (HK1, C666-1 and HK1_EBV), which showed inactivation of *RERG*, was transfected with the pCMV6-*RERG* plasmid or the empty-vector pCMV6-Entry plasmid using Fugene HD (Promega). After 48 h, cells were harvested for further experiments and selected with G418 (400 μg/mL; Millipore, Darmstadt, Germany) for 2 weeks to obtain

stably transfected cell lines. Transfected cell lines were verified by qRT-PCR and western blotting. The stable cells were maintained in medium containing 200 μg/mL G418.

Cell proliferation assay

The effect of *RERG* on NPC cell proliferation was measured using an MTT assay or a CCK8 assay. NPC cells transfected with empty vector or *RERG* vector were seeded in 96-well plates at a proportionate density and incubated at 37°C. Subsequently, cell proliferation was assessed every 24 h for the indicated duration. Briefly, 10 μL of MTT (3-(4,5-dimethylthiazol-2-yl)-2,5-diphenyl tetrazolium bromide, 5.0 mg/mL; Sigma-Aldrich) or CCK8 (cell counting kit-8, Dojindo Laboratories, Kumamoto, Japan) was added to each well, and the plates were incubated for 4 h at 37°C. Optical density (OD) was determined at 570 nm (MTT assay) or 450 nm (CCK8 assay) on a Bio-Rad model 680 microplate reader (Bio-Rad Laboratories, Hercules, CA, USA). OD values reflect the relative number of viable cells.

Colony formation assay

HK1 cells stably expressing *RERG* or empty vector and HK1_EBV cells transfected with *RERG* or empty vector after 48 h were counted and plated at 500 cells/dish into 60-mm dishes. Then cells were incubated at 37°C and at an atmosphere of 5% CO_2 for 2 weeks. Once the cells formed visible colonies, the colonies were washed twice with phosphate-buffered saline and fixed with 70% ethanol for 20 min. The cells were appropriately stained with Giemsa's solution (Merck, Darmstadt, Germany) and allowed to air dry at room temperature. The experiments were triplicated and the numbers of colonies were microscopically counted.

In vitro cell migration and invasion assay

Cell migration assays were performed using the CytoSelect Cell Migration Assay kit

(membrane filter pore size, 8 μm; Cell BioLabs, San Diego, CA, USA). Cell invasion assays were performed using the CytoSelect 24-Well Cell Invasion Assay (basement membrane, membrane filter pore size, 8 μm; Cell BioLabs). HK1 cells stably expressing *RERG* or empty vector were suspended (0.15×10^6 transfected cells/well) in serum-free medium and placed in the upper chamber, and media containing 10% FBS was placed in the lower well of the migration or invasion plate. After incubation for 24 h and removal of non-migratory cells or non-invasive cells, cells that migrated or passed through the filter were stained, photographed, and counted under a microscope (magnification, ×100 and ×200) for each filter in 3 areas.

In vivo tumorigenicity assay

Male BALB/c athymic nu/nu mice (5-week-old) (weight range: 17–19 g; Japan SLC, Hamamatsu, Japan) were used to examine tumorigenicity in vivo. The animal experiments were performed according to the Mie University guidelines for laboratory animals (approval No. 26–19). Nude mice were housed in ventilated caging conditions under a 12-h dark/light cycle at constant humidity and temperature. Animals were permitted free access to sterile water and standard laboratory chow. HK1 cells (2×10^6 cells/mouse) stably transfected with *RERG* were injected subcutaneously into the left flank near the forelimb or an equal number of empty vector stable transfected HK1 cells were injected into the right flank. Tumor growth was measured every 3 days for 3 weeks. Tumor volume (mm^3) was calculated with a caliper (model 530–312; range 0–150 mm; Mitutoyo, Kawasaki, Japan) and evaluated using the formula: $V=L \times W \times H \times \pi/6$, where L, W, and H represent tumor diameter in 3 mutually perpendicular planes. Mice were sacrificed by cervical dislocation at the third week after subcutaneous injection. Tumor grafts were then excised and weighed. The tumors were kept in 4% formamide and

RNAlater solution for further analysis of IHC and mRNA expression levels, respectively.

Western blot analysis

Western blot was done according to the standard protocol as described previously.[31] Cultured cells were harvested at 70-80% confluence and lysed using RIPA buffer (Cell Signaling Technology Inc., Dancers, MA, USA) supplemented PMSF (Phenylmethylsulfonyl fluoride, NACALAI TESQUE, INC., Kyoto, Japan). The list of antibodies used in this study is summarized in Additional file 1: Table S1. Signals were detected by LAS4000mini (Fujifilm, Tokyo, Japan), and band intensities of western blots were quantitatively measured integrated grayscale densities in windows of identical size incorporating for each band using ImageJ software (ver. 1.48).

IHC staining, immunocytochemistry (ICC) staining, and double immunofluorescence staining

For IHC and ICC analysis, standard immunoperoxidase methods were performed as previously described.[29] The list of antibodies used in this study were summarized in Table S1. IHC grading based on intensity and frequency of staining was performed by 2 independent investigators. Staining intensity was scored as negative (0), weak (+1), moderate (+2), or strong (+3). The frequency of positive cells in specific areas was scored as negative (0), less than 25% (+1), 25–50% (+2), 51–75% (+3), or more than 75% (+4), as previously published.[32] The number of cells staining positively for ICC was analyzed using ImageJ software (ver. 1.48).

For immunofluorescence analysis, after deparaffinization and rehydration, antigen was retrieved in 5% urea buffer by microwave heating for 5 min. Sections of 3-μm thickness were incubated overnight at room temperature with the following antibodies: rabbit polyclonal

anti-α-SMA (1:200, Abcam, Cambridge, UK) and mouse monoclonal anti-CD34 (1:200, Monosan, Uden, Netherlands). The sections were next incubated with the following fluorescent secondary antibodies at 1:400 each for 2 h at room temperature (Molecular Probes, Eugene, OR, USA: Alexa 488-labeled goat anti-rabbit IgG antibody; Alexa 594-labeled goat anti-mouse IgG antibody). Finally, the nuclei were stained with 4',6-diamidino-2-phenylindole (DAPI) and the sections were examined with a fluorescence microscope (BX53, Olympus, Tokyo, Japan).

For digital microscopy assessment of microvessel density, the intensity and area of endothelial or periendothelial cell staining were quantitatively measured using ImageJ software (ver. 1.48). The proportion of blood vessels exhibiting endothelial (CD34-positive) or periendothelial (α-SMA-positive) cells was defined as the area fraction (%) at a magnification of ×200.

Statistical analysis

All statistical analyses were performed with SPSS v16.0 (SPSS, Chicago, IL, USA). The unpaired Student's t-test was used to compare the average of 2 groups, and the paired Student's t-test was used to compare the size and weight of tumor xenografts in the left and right flanks of nude mice. Statistical differences between IHC scores were determined by the Mann-Whitney U test. Receiver operating characteristic (ROC) curves were generated to confirm the accuracy of diagnosis by *RERG* methylation rate, and sensitivity and specificity were computed. $P < 0.05$ was considered as statistically significant.

Results

RERG is down-regulated and hypermethylated in NPC primary tumors

We performed the methyl-DNA binding domain capture technique and cDNA

microarray analysis in seven NPC patients compared to five NNE patients (unpublished data). In the cDNA microarray, 5 genes of RAS type GTPase family were found to be significantly altered. Among these, 3 genes decreased under half and 2 genes increased more than two-fold compared to the NNE group (Additional file 2: Figure. S1A). In the Methylated-DNA capture sequencing data, 8 genes of RAS type GTPase family that have an increased more than two-fold level of CpG island methylation relative to NNE group (Additional file 2: Figure. S1B). *RERG*, *RASL11A* and *RASL11B* were marked with DNA promoter methylation and downregulated in NPC tissues (Additional file 2: Figure. S1C). *RERG* gene expression was most significantly decreased in cDNA microarray and highly methylated in NPC, which we chose it for our further study.

We evaluated the expression levels of RERG in NPC primary tumors by qRT-PCR and IHC staining. *RERG* expression was significantly lower in NPC primary tumors than NNE tissues (Fig. 1a). IHC staining was then performed to evaluate the expression of RERG proteins in NPC patients and NNE subjects. Moderate expression of RERG (Fig. 1b) was observed in the membrane and cytoplasm of normal nasopharyngeal epithelium cells, while very weak or no expression of RERG was observed in NPC cancer nests. The IHC score of NPC tissues was significantly lower than that of NNE tissues (Fig. 1b). These results suggest that RERG is down-regulated in NPC primary tumors.

A genome database, accessed using the UCSC Genome Browser (https://genome.ucsc.edu/), revealed that the *RERG* promoter contains a CpG island (CGI). As CGI methylation is a well-recognized epigenetic mechanism of TSGs silencing in cancer [33], we sought to determine the quantitation of methylation at the promoter of *RERG*. We performed

methyl qPCR in 46 NPC patients and 13 NNE subjects (Fig. 1c). The methylation rate of *RERG* promoter was significantly higher in the NPC group (Average 32.6 %) than in the no-cancer group (1.0 %) (Fig. 1d, $P<0.001$).

In addition, ROC curves was conducted to evaluate whether the methylation of *RERG* could be used to be a potential marker for screening NPC. The area under the curve (AUC) of ROC plots for *RERG* methylation rate in the detection of NPC was 0.897 (95%CI: 0.818–0.976) (Fig. 1e). At a meth-index cutoff value of 5.2 %, the methylation rate of *RERG* gave 78.3% sensitivity and 100% specificity. The current results indicated that DNA methylation rate of *RERG* holds some promise for NPC screening.

RERG is silenced in NPC cell lines with DNA hypermethylation and restored by pharmacologic demethylation

We also investigated the mRNA expression of *RERG* in cell lines. *RERG* was found to be silenced to a greater extent in NPC cell lines HK1, C666-1 and HK1_EBV compared to an immortalized epithelial cell line (NP460) (Fig. 2a).

We then determined the methylation rate of *RERG* promoter in cell lines. As expected, *RERG* was highly methylated in all 3 NPC cell lines compared to the immortalized normal epithelial cell line, NP460 (Fig. 2b). To further investigate methylation status, we used BGS to determine 25 individual CpG sites from -145 to +133 bp from the transcription start site of the *RERG* promoter. All 25 CpG sites were obviously methylated in NPC cell lines (HK1 and C666-1), but were seldom methylated in the normal cell line, NP460 (Fig. 2c). These results indicate that *RERG* methylation is a common event in NPC.

To investigate whether CpG methylation directly mediates *RERG* down-regulation, 3

NPC cell lines were treated with the DNA methyltransferase inhibitor Aza either alone or in combination with the HDAC inhibitor TSA (A + T). We found that *RERG* expression levels were significantly restored after the demethylation treatment (Fig. 2d), suggesting that promoter methylation might contribute to the silencing of *RERG* in NPC cells. In addition, the mRNA expression levels of *RERG* were up-regulated in demethylated HK1 (2.0 and 1.85 fold with Aza alone and Aza + TSA, respectively) and C666-1 cells (0.57 and 0.62 fold with Aza alone and Aza + TSA, respectively) closed to the immortalized epithelial cell line NP460. *RERG* was highly up-regulated in demethylated HK1_EBV (8.66 and 11.51 fold with Aza alone and Aza + TSA, respectively) than NP460.

Overexpression of RERG suppresses cell proliferation, clonogenicity, migration and invasion

To assess the biological roles of RERG in NPC cells, we performed transfection of *RERG*-expression vector in 3 NPC cell lines (HK1, C666-1 and HK1_EBV). We established one stable RERG-expressing HK1 cells. The overexpression of RERG was confirmed by western blot (Fig. 3a, inset). Overexpression of RERG significantly inhibited NPC cell proliferation (Fig. 3a). Moreover, the proliferative effect of RERG was confirmed via ICC staining of PCNA, a marker of cell proliferation in HK1 stable cells. The number of PCNA-positive cells was significantly reduced by 15% in HK1-RERG cells (Fig. 3b). RERG also significantly reduced the colony formation (Fig. 3c), migration efficiency (Fig. 3d) and invasion (Fig. 3e) of NPC cells, when compared with empty-vector cells.

Overexpression of RERG suppresses MMPs and pro-angiogenic factors via the ERK and NF-κB signaling pathway in NPC cells

To explore the mechanism of tumor suppression by RERG, we compared the expression levels of major ERK and NF-κB signaling pathway members, prominent cell migration and invasion molecules (MMP-2 and MMP-9), and several pro-angiogenesis-related factors, such as vascular endothelial growth factor (VEGF), IL8 and IL6 in NPC cells. RERG reduced p-ERK and p-p65, and increased p-IKBα protein levels in NPC cell lines, as typically seen in HK1 stable cells and C666-1 cells (Fig. 4a). Also, MMPs were suppressed by the overexpression of RERG (Fig. 4b). The significant downregulation of IL8 and IL6 were confirmed in HK1 stable cell by western blotting (Fig. 4c). However, RERG showed limited effects on VEGF when compared to empty-vector cells (Fig. S2A). As expected, RERG suppressed ERK and NF-κB signaling pathway and its downstream effectors. It has been reported that both Ras/ERK and NF-κB signaling are significantly associated with cell proliferation, survival, differentiation, and commonly involved in malignant transformation in a variety of human cancers.[34] Thus, these results suggested that RERG overexpression exerted a tumor suppressor role by attenuating the activation of ERK/NF-κB signaling pathway.

Overexpression of RERG suppresses tumorigenesis and angiogenesis in vivo

We further tested whether RERG is able to suppress the growth of NPC cells in vivo. Stable transfected HK1-RERG and HK1-Empty cells formed tumors in nude mice. A 100% tumor formation rate suggested that *RERG* did not affect tumor incidence in vivo. However, the subcutaneous tumor growth curve was significantly less steep for *RERG*-transfected cells than for controls (Fig. 5a). After 19 days, xenografts were removed from mice (Figs. 5b). The mean weight of tumors formed by *RERG*-transfected cells was significantly lower than that of controls (59.2 ± 17.3 mg vs 254.6 ± 84.9 mg; Fig. 5c), indicating that RERG can inhibit NPC

tumorigenicity in vivo.

RERG expression was confirmed by IHC (Fig. 5d, e) and qRT-PCR (Additional file 3: Figure. S2B). In a histopathological analysis, H&E staining showed that angiogenesis was suppressed in xenografts from the RERG group (Fig. 5d). To study the potential effect of RERG on angiogenesis, the development of microvessels in tumor sections of nude mice was examined by immunofluorescence staining with vascular endothelial cell marker CD34 and periendothelial cell marker α-SMA (Fig. 5d). Area fraction of CD34 and α-SMA was significantly lower in the mouse xenografts within the RERG-overexpressed tumors (Fig. 5e).

RERG mediates downregulation of MMPs and pro-angiogenic cytokines with the inhibition of NF-κB signaling

The NF-κB signaling pathway is known to promote tumor progression and angiogenesis.[24, 25] To understand how NF-κB signaling pathway is regulated by RERG in vivo, we focused on the subunit p65 translocation into the cell nuclei. IHC staining indicated that p-p65 localized exclusively in the nuclei of control mouse xenografts and slightly in the RERG-overexpressed mouse xenografts tumors (Fig. 6a). Interestingly, a decrease in total p65 expression was also observed in RERG-overexpressed tumors (Fig. 6a). It is indicated that expression of RERG inhibited p65 nuclear translocation in vivo. We then confirmed pro-angiogenic cytokines (IL8 and IL6), TIMP-2, and MMPs (MMP-2 and MMP-9) in the isolated tumor tissues by IHC (Fig. 6a). Pro-angiogenic cytokines IL8 and IL6 were significantly downregulated in RERG-overexpressed tumors (Fig. 6b). IHC scores (Fig. 6b) indicated that overexpression of RERG significantly decreased the expression of MMPs (MMP-2 and MMP-9), and drastically up-regulated TIMP-2, which is an inhibitor of MMPs, including MMP-2 and

MMP-9. Real-time qRT-PCR validated that the mRNA expression of *IL8* and *IL1β* were downregulated by *RERG* in mouse xenografts tumors (Additional file 3: Figure. S2B). On the other hand, the expression of TNFα and VEGF showed no significant changes in vivo (Additional file 3: Figure. S2B, C). These results suggested that RERG efficiently inhibited the cell proliferation, migration, invasion and angiogenesis of NPC cells by suppressing the cell migratory and pro-angiogenic molecules (MMP-2, MMP-9, IL8, IL6 and IL1β) via the ERK/NF-κB signaling pathway (Fig. 6c), but not VEGF and TNFα.

Discussion

In this study, we found that *RERG* was frequently silenced in NPC tissues and cell lines. As mRNA expression of *RERG* was pharmacologically reversible, promoter methylation seems to be the major mechanism of inactivating *RERG*, and histone modification may partly co-enhance its demethylation effect. Epigenetic gene silencing is associated with the onset and progression of various cancers.[7] The frequent, predominant epigenetic inactivation of *RERG* in NPC points to the importance of this gene in tumorigenesis. We also found that *RERG* exerts its tumor suppressor functions by inhibiting ERK/NF-κB signaling pathway, resulting in suppression of tumor cell proliferation, clonogenicity, migration, invasion and angiogenesis (Fig. 6c). These results suggest that RERG suppresses cellular growth through signaling pathways in which these molecules participate. Although this and other studies have demonstrated that RERG is down-regulated in multiple cancers, few studies have reported on its function and related mechanisms in tumorigenesis. To the best of our knowledge this study is the first to reveal the underlying antitumor mechanisms of RERG in NPC.

RERG is a member of RAS GTPase superfamily, which had previously been implicated

regulating Ras/MEK/ERK signaling pathway activation.[12] The Ras/MEK//ERK pathway, one of mitogen-activated protein kinases (MAPKs), function in a variety of cellular regulation leading to cell growth and development, and is hyperactivated in a variety of human cancers[34], such as gastric adenocarcinoma, hepatocarcinoma, colon cancer[35, 36] and NPC.[37] Phosphorylation of ERK proteins via the Ras/MEK/ERK signaling pathway cascade induces the activation of transcription factors NF-κB, AP-1, and ETS.[20] NF-κB is also a well-known master regulator of host inflammatory responses and NF-κB activation is a common event in human cancers, including NPC.[38] Activation of NF-κB influences the proliferation, survival, invasive, and metastatic properties of cancer cells by regulating the transcription of various important target genes.[39] Our results indicate that overexpression of RERG inhibited ERK/NF-κB in several NPC cell lines, and reduced total p65 and activated p65 both in vitro and in vivo. Several reports indicated that the inhibition of NF-κB activity in NPC cells resulted in the down-regulation of downstream target genes such as MMPs and IL8.[40, 41] Therefore, it is conceivable that RERG affects the ERK/NF-κB signaling pathway in NPC cells.

The tumor microenvironment, composed of non-cancer cells and their stroma, influences on metastasis as a dynamic process[42] and angiogenesis response to a tumor.[43] Various of pro-tumorigenic factors, including MMPs and cytokines are produced by tumor cells as well as by the tumor stroma. MMPs, a family of zinc metallo-endopeptidases capable of digesting the extracellular matrix and basement membrane, promote tumor invasion and metastasis.[44] Decreased MMP expression and activity can inhibit cancer cell adhesion, migration, invasion and angiogenesis. In this study, we confirmed that ectopic expression of RERG reduced MMP-2 and MMP-9 expression in vitro and in vivo, although some differences were observed

between the results of in vitro and in vivo. In mouse xenografts tumors model, the MMPs can be secreted by cancer cells as well as cancer-associated fibroblasts (CAF). The crosstalk between cancer cells and tumor stroma in the tumor microenvironment enhances the production of pro-angiogenic protein, including MMPs. A possible explanation is that overexpression of RERG might suppress the crosstalk between cancer cells and tumor stroma in vivo, but not in vitro. Additionally, IHC showed that TIMP-2, an inhibitor of MMPs, was up-regulated in mouse xenografts. It was reported that TIMPs exert antiangiogenic activity by suppressing MMPs or by directly inhibiting endothelial cell proliferation.[45] An imbalance between MMPs and TIMPs might result in the deposition or degradation of the extracellular matrix.[46] In the present study, therefore, we speculated that the overexpression of RERG mediated the suppression of ERK/NF-κB pathway, reducing the expression of MMP-2 and MMP-9 in NPC. These results might provide a molecular basis for its ability to inhibit cell proliferation, migration and invasion.

In addition, we observed that in a mouse xenograft model, RERG inhibited microvessel development as well as tumor growth. CD34 (an endothelial cell marker) and α-SMA (a pericyte marker) was dramatically decreased in the mouse xenografts within the RERG-expression. Our previous IHC study suggested that α-SMA-positive stromal cells may recruit circulating endothelial progenitor cells into NPC stroma for angiogenesis.[32] As α-SMA is widely accepted as CAF marker, there is a possibility of the activation and the recruitment of the stromal cells, and it may be inhibited by the over-expression of the novel tumor suppressor gene (*RERG*). As overexpression of RERG reduced the expression of α-SMA in mouse xenograft model, it is suggested that RERG might involve in the suppressing the crosstalk

between tumor cells and tumor microenvironment.

Angiogenesis is a highly regulated process involving sprouting from pre-existing vessels and maturation into new blood vessels.[47] It can be triggered and modified by various factors, including cytokines, growth factors and their receptors, chemokines, and matrix metalloproteinases.[47] However, there are no studies on the relationship between angiogenesis and RERG. VEGF is one of the most well-known pro-angiogenic factors, stimulating the sprouting and proliferation of endothelia cells.[43] IL8 is a pro-angiogenesis cytokine, which may promote both tumor growth and the formation of new blood vessels.[48, 49] IL6 promotes the migration and invasion in NPC cell lines and mediated through regulation of the expression of MMP-2 and MMP-9.[50] IL-1 α and β were detectable in the majority of primary NPC biopsies and a fraction of metastatic lesions and its absence in control nasopharyngeal tissues.[51] In this study, RERG decreased IL8, IL6 and IL1β expression and angiogenesis in tumor xenografts in nude mice. In addition, the protease MMPs were well-known pro-angiogenic factors in the angiogenesis pathway.[43, 52, 53] RERG increased the expression of TIMP-2 and inhibited the expression of MMP-2 and MMP-9, providing support for a mechanistic explanation of the inhibition of tumor microvessel growth and size by RERG. MMPs, as well as cytokines, IL8 and IL6 were the most down-regulated pro-angiogenic factors, followed re-expression of RERG in NPC. However, the effect of VEGF and TNFα were not significant, indicating that they may not play important roles in suppressing angiogenesis via RERG regulation. This study provides the first evidence that RERG expression can reduce angiogenesis. In this study, we observed that RERG reduced cellular migration and invasion in NPC in vitro and suppressed tumor growth and angiogenesis in vivo, but the potential ability and the detailed mechanisms

of RERG-inducing distant metastasis in vivo requires further study.

Conclusions

We demonstrated that *RERG* functioned as a TSG through suppression of ERK/NF-κB signaling pathway, and was frequently silenced by promoter CpG methylation in NPC. This study provides insights into the possible mechanisms underlying the role of RERG in NPC carcinogenesis, and suggests that RERG might be employed as a target molecule in cancer therapy.

Acknowledgments

This work was supported by grant from Japan Society for the Promotion of Science (KAKENHI JP22406016, JP25305020, JP16H05829). This work was also supported by the National Natural Science Foundation of China (81272983) and Guangxi Natural Science Foundation (2013GXNSFGA019002).

Availability of data and materials

All data analyzed during this study are included in this published article. Raw and processed data are stored in the laboratory of the corresponding authors and are available upon request.

Authors' contributions

MM and KT conceived the project and planned experiments. WLZ, NM, YXM and SMW performed experiments and analyzed the data. KM contributed to data analysis. MM, KM and WLZ wrote the manuscript. YH, SO, GWH and ZZ critically read the manuscript, directed and supervised experiments. All authors read and approved the final manuscript.

Competing interests

The authors declare that they have no competing interests.

Funding

See acknowledgments.

Consent for publication

No individual person's data in any form were involved in this study.

Ethical approval and consent to participate

This study was approved by the ethical review committees of the First Affiliated Hospital of Guangxi Medical University, China (2009-07-07), and Mie University Graduate School of Medicine, Japan (no.1116).

Author details

[1]Department of Environmental and Molecular Medicine, Mie University Graduate School of Medicine, Tsu, Mie, Japan,

[2]Department of Otolaryngology Head and Neck Surgery, Mie University Graduate School of Medicine, Tsu, Mie, Japan,

[3]Department of Otolaryngology Head and Neck Surgery, First Affiliated Hospital of Guangxi Medical University, Nanning, Guangxi, China,

[4]Graduate School of Health Science, Suzuka University of Medical Science, Suzuka, Mie, Japan

Reference:

1. Tao Q, Chan AT. Nasopharyngeal carcinoma: molecular pathogenesis and therapeutic developments. Expert Rev Mol Med 2007;9(12): 1-24.
2. Lo AK, Lo KW, Tsao SW, et al. Epstein-Barr virus infection alters cellular signal cascades in human nasopharyngeal epithelial cells. Neoplasia 2006;8(3): 173-80.
3. Wei WI, Mok VW. The management of neck metastases in nasopharyngeal cancer. Curr Opin Otolaryngol Head Neck Surg 2007;15(2): 99-102.
4. Suva ML, Riggi N, Bernstein BE. Epigenetic reprogramming in cancer. Science 2013;339(6127): 1567-70.
5. Egger G, Liang G, Aparicio A, et al. Epigenetics in human disease and prospects for epigenetic therapy. Nature 2004;429(6990): 457-63.
6. Baylin SB, Jones PA. A decade of exploring the cancer epigenome - biological and translational implications. Nat Rev Cancer 2011;11(10): 726-34.
7. Baylin SB, Ohm JE. Epigenetic gene silencing in cancer - a mechanism for early oncogenic pathway addiction? Nat Rev Cancer 2006;6(2): 107-16.
8. Feinberg AP, Ohlsson R, Henikoff S. The epigenetic progenitor origin of human cancer. Nat Rev Genet 2006;7(1): 21-33.
9. Lo KW, Huang DP. Genetic and epigenetic changes in nasopharyngeal carcinoma. Semin Cancer Biol 2002;12(6): 451-62.
10. Zhang Z, Sun D, Hutajulu SH, et al. Development of a non-invasive method, multiplex methylation specific PCR (MMSP), for early diagnosis of nasopharyngeal carcinoma. PLoS One 2012;7(11): e45908.

11. Tian F, Yip SP, Kwong DL, et al. Promoter hypermethylation of tumor suppressor genes in serum as potential biomarker for the diagnosis of nasopharyngeal carcinoma. Cancer Epidemiol 2013;37(5): 708-13.

12. Finlin BS, Gau CL, Murphy GA, et al. RERG is a novel ras-related, estrogen-regulated and growth-inhibitory gene in breast cancer. J Biol Chem 2001;276(45): 42259-67.

13. Sorlie T, Perou CM, Tibshirani R, et al. Gene expression patterns of breast carcinomas distinguish tumor subclasses with clinical implications. Proc Natl Acad Sci U S A 2001;98(19): 10869-74.

14. Key MD, Andres DA, Der CJ, et al. Characterization of RERG: an estrogen-regulated tumor suppressor gene. Methods Enzymol 2006;407: 513-27.

15. Habashy HO, Powe DG, Glaab E, et al. RERG (Ras-like, oestrogen-regulated, growth-inhibitor) expression in breast cancer: a marker of ER-positive luminal-like subtype. Breast Cancer Res Treat 2011;128(2): 315-26.

16. Oster B, Thorsen K, Lamy P, et al. Identification and validation of highly frequent CpG island hypermethylation in colorectal adenomas and carcinomas. Int J Cancer 2011;129(12): 2855-66.

17. Luo X, Huang R, Sun H, et al. Methylation of a panel of genes in peripheral blood leukocytes is associated with colorectal cancer. Sci Rep 2016;6: 29922.

18. Ho JY, Hsu RJ, Liu JM, et al. MicroRNA-382-5p aggravates breast cancer progression by regulating the RERG/Ras/ERK signaling axis. Oncotarget 2017;8(14): 22443-59.

19. Cao Y, Liang H, Zhang F, et al. Prohibitin overexpression predicts poor prognosis and promotes cell proliferation and invasion through ERK pathway activation in gallbladder

cancer. J Exp Clin Cancer Res 2016;35: 68.

20. Bancroft CC, Chen Z, Dong G, et al. Coexpression of proangiogenic factors IL-8 and VEGF by human head and neck squamous cell carcinoma involves coactivation by MEK-MAPK and IKK-NF-kappaB signal pathways. Clin Cancer Res 2001;7(2): 435-42.

21. Zhang J, Wen X, Ren XY, et al. YPEL3 suppresses epithelial-mesenchymal transition and metastasis of nasopharyngeal carcinoma cells through the Wnt/beta-catenin signaling pathway. J Exp Clin Cancer Res 2016;35(1): 109.

22. Meng DF, Xie P, Peng LX, et al. CDC42-interacting protein 4 promotes metastasis of nasopharyngeal carcinoma by mediating invadopodia formation and activating EGFR signaling. J Exp Clin Cancer Res 2017;36(1): 21.

23. Miyake M, Goodison S, Lawton A, et al. Angiogenin promotes tumoral growth and angiogenesis by regulating matrix metallopeptidase-2 expression via the ERK1/2 pathway. Oncogene 2015;34(7): 890-901.

24. Basseres DS, Baldwin AS. Nuclear factor-kappaB and inhibitor of kappaB kinase pathways in oncogenic initiation and progression. Oncogene 2006;25(51): 6817-30.

25. Richmond A. Nf-kappa B, chemokine gene transcription and tumour growth. Nat Rev Immunol 2002;2(9): 664-74.

26. Tsang CM, Zhang G, Seto E, et al. Epstein-Barr virus infection in immortalized nasopharyngeal epithelial cells: regulation of infection and phenotypic characterization. Int J Cancer 2010;127(7): 1570-83.

27. Huang DP, Ho JH, Poon YF, et al. Establishment of a cell line (NPC/HK1) from a

differentiated squamous carcinoma of the nasopharynx. Int J Cancer 1980;26(2): 127-32.

28. Li HM, Man C, Jin Y, et al. Molecular and cytogenetic changes involved in the immortalization of nasopharyngeal epithelial cells by telomerase. Int J Cancer 2006;119(7): 1567-76.

29. Wang S, Mo Y, Midorikawa K, et al. The potent tumor suppressor miR-497 inhibits cancer phenotypes in nasopharyngeal carcinoma by targeting ANLN and HSPA4L. Oncotarget 2015;6(34): 35893-907.

30. Mo Y, Midorikawa K, Zhang Z, et al. Promoter hypermethylation of Ras-related GTPase gene RRAD inactivates a tumor suppressor function in nasopharyngeal carcinoma. Cancer Lett 2012;323(2): 147-54.

31. Wang S, Ma N, Zhao W, et al. Inflammation-Related DNA Damage and Cancer Stem Cell Markers in Nasopharyngeal Carcinoma. Mediators Inflamm 2016;2016: 9343460.

32. Wang S, Ma N, Kawanishi S, et al. Relationships of alpha-SMA-positive fibroblasts and SDF-1-positive tumor cells with neoangiogenesis in nasopharyngeal carcinoma. Biomed Res Int 2014;2014: 507353.

33. Jones PA, Baylin SB. The fundamental role of epigenetic events in cancer. Nat Rev Genet 2002;3(6): 415-28.

34. Dhillon AS, Hagan S, Rath O, et al. MAP kinase signalling pathways in cancer. Oncogene 2007;26(22): 3279-90.

35. Ding C, Luo J, Li L, et al. Gab2 facilitates epithelial-to-mesenchymal transition via the MEK/ERK/MMP signaling in colorectal cancer. J Exp Clin Cancer Res 2016;35: 5.

36. Giordano G, Febbraro A, Tomaselli E, et al. Cancer-related CD15/FUT4 overexpression decreases benefit to agents targeting EGFR or VEGF acting as a novel RAF-MEK-ERK kinase downstream regulator in metastatic colorectal cancer. J Exp Clin Cancer Res 2015;34: 108.

37. Tulalamba W, Janvilisri T. Nasopharyngeal carcinoma signaling pathway: an update on molecular biomarkers. Int J Cell Biol 2012;2012: 594681.

38. Chung GT, Lou WP, Chow C, et al. Constitutive activation of distinct NF-kappaB signals in EBV-associated nasopharyngeal carcinoma. J Pathol 2013;231(3): 311-22.

39. Ghosh S, Hayden MS. Celebrating 25 years of NF-kappaB research. Immunol Rev 2012;246(1): 5-13.

40. Lin ML, Lu YC, Chung JG, et al. Down-regulation of MMP-2 through the p38 MAPK-NF-kappaB-dependent pathway by aloe-emodin leads to inhibition of nasopharyngeal carcinoma cell invasion. Mol Carcinog 2010;49(9): 783-97.

41. Ren Q, Sato H, Murono S, et al. Epstein-Barr virus (EBV) latent membrane protein 1 induces interleukin-8 through the nuclear factor-kappa B signaling pathway in EBV-infected nasopharyngeal carcinoma cell line. Laryngoscope 2004;114(5): 855-9.

42. Quail DF, Joyce JA. Microenvironmental regulation of tumor progression and metastasis. Nat Med 2013;19(11): 1423-37.

43. Weis SM, Cheresh DA. Tumor angiogenesis: molecular pathways and therapeutic targets. Nat Med 2011;17(11): 1359-70.

44. Curran S, Murray GI. Matrix metalloproteinases: molecular aspects of their roles in tumour invasion and metastasis. Eur J Cancer 2000;36(13 Spec No): 1621-30.

45. Jiang Y, Goldberg ID, Shi YE. Complex roles of tissue inhibitors of metalloproteinases in cancer. Oncogene 2002;21(14): 2245-52.

46. Yeh CB, Hsieh MJ, Hsieh YH, et al. Antimetastatic effects of norcantharidin on hepatocellular carcinoma by transcriptional inhibition of MMP-9 through modulation of NF-kB activity. PLoS One 2012;7(2): e31055.

47. Gupta MK, Qin RY. Mechanism and its regulation of tumor-induced angiogenesis. World J Gastroenterol 2003;9(6): 1144-55.

48. Lo MC, Yip TC, Ngan KC, et al. Role of MIF/CXCL8/CXCR2 signaling in the growth of nasopharyngeal carcinoma tumor spheres. Cancer Lett 2013;335(1): 81-92.

49. Sparmann A, Bar-Sagi D. Ras-induced interleukin-8 expression plays a critical role in tumor growth and angiogenesis. Cancer Cell 2004;6(5): 447-58.

50. Sun W, Liu DB, Li WW, et al. Interleukin-6 promotes the migration and invasion of nasopharyngeal carcinoma cell lines and upregulates the expression of MMP-2 and MMP-9. Int J Oncol 2014;44(5): 1551-60.

51. Huang YT, Sheen TS, Chen CL, et al. Profile of cytokine expression in nasopharyngeal carcinomas: a distinct expression of interleukin 1 in tumor and CD4+ T cells. Cancer Res 1999;59(7): 1599-605.

52. Kessenbrock K, Plaks V, Werb Z. Matrix metalloproteinases: regulators of the tumor microenvironment. Cell 2010;141(1): 52-67.

53. Gialeli C, Theocharis AD, Karamanos NK. Roles of matrix metalloproteinases in cancer progression and their pharmacological targeting. FEBS J 2011;278(1): 16-27.

Figure legends

Figure 1. RERG was down-regulated and hypermethylated in NPC primary tumors. a Expression levels of *RERG* were measured in NPC primary tumor biopsies (n=16) and NNE tissues (n=13) by qRT-PCR. *GAPDH* was used as an internal control. **: $P < 0.01$ analyzed by Student's t-test. **b** RERG was down-regulated in NPC clinical samples (n=13) compared to NNE epithelium (n=9) by IHC. Left: Representative photographs of IHC analyses of the expression of RERG. Original magnification is ×200, inner enlarged magnification is ×400. Bar represents 50 μm and 20 μm, respectively. Right: Graphs represent means ± SD of IHC scores of RERG in tissues of NPC and NNE. *: $P < 0.05$ by Mann-Whitney U test. **c** Each methylation rate (%) of *RERG* in NPC clinical samples and NNE samples by methyl qPCR. **d** Means ± SD of methylation rates of *RERG* in NPC group (n=46) and NNE group (n=13). ***: $P < 0.001$ by Student's t-test. **e** ROC analysis of DNA methylation index of *RERG*.

Figure 2. *RERG* was down-regulated and hypermethylated in NPC cell lines, and restored by pharmacologic demethylation. a Gene expression was detected in tumor cell lines (HK1, C666-1, HK1_EBV) and an immortalized normal epithelia NP460 cells (n=4) by qRT-PCR. *GAPDH* was used as an internal control. **b** *RERG* was highly methylated in NPC cell lines (HK1, C666-1, HK1_EBV) compared to NP460 (n=3) by methyl qPCR. **c** Bisulfite genomic sequencing of the 25 CpG sites within the RERG promoter region in 2 NPC cell lines (HK1 and C666-1) and an immortalized epithelial cell line (NP460). Five clones were randomly selected and sequenced for each sample. Each row represents analysis of an individual promoter allele. Open circles indicate unmethylated cytosines, and filled circles indicate

methylated cytosines. **d** *RERG* expression of NP460 and NPC cell lines (n=3) treated with 5-aza-2'-deoxycytidine (Aza) alone or combined with trichostatin A (TSA) (A + T) were determined by qRT-PCR. *GAPDH* was used as an internal control. *: $P < 0.05$, **: $P < 0.01$, ***: $P < 0.001$ analyzed by Student's t-test.

Figure 3. Overexpression of RERG inhibited cell proliferation, colony formation, migration and invasion. **a** Growth curves of *RERG*-transfected and empty-vector-transfected NPC cells (HK1, C666-1, HK1_EBV). Data are means ± SD (n=5). The insets show protein levels of RERG in each cell line transfected with empty and *RERG* vector. **b** ICC staining of HK1 stable cells against PCNA (magnification, ×200). PCNA-positive percentages in cultured HK1-RERG cells and HK1-empty cells (control) are presented as means ± SD (n=4). **c** Colony formation assays. Cell colonies were stained with Giemsa. Quantitative analyses of colony formation efficiency show the means ± SD (n=3) of at least 2 independent experiments. **d** Migration assay. Cells were seeded in a migration chamber and cultured for 24 h. Migratory cells were stained, photographed under a microscope and quantitatively analyzed. **e** Invasion assay. Cells were seeded in an upper chamber and cultured for 24 h. Invasive cells were stained, photographed under a microscope and quantitatively analyzed. Data are shown as means ± SD (n=3) of at least 2 independent experiments. *: $P < 0.05$, **: $P < 0.01$, ***: $P < 0.001$ by Student's t-test.

Figure 4. RERG suppressed ERK/NF-κB signaling pathway and expression of MMPs, IL8 and IL6 in NPC cells. Protein levels of (**a**) ERK/NF-κB signaling effectors and (b) MMP2

and MMP9 in *RERG*-transfected and empty-vector-transfected NPC cells (HK1, C666-1, HK1_EBV) were determined by western blotting (n=3). **c** IL8 and IL6 in *RERG*-transfected and empty-vector-transfected NPC cells (HK1) were determined by western blotting (n=3). Data are shown as means ± SD. *: $P < 0.05$, **: $P < 0.01$, ***: $P < 0.001$ by Student's t-test.

Figure 5. RERG inhibited the tumorigenesis and angiogenesis of NPC in vivo. Eight male BALB/c athymic nu/nu mice injected with 2×10^6 cells. **a** Growth curve of tumors in nude mice. Tumor volume was measured every 3 days after inoculation. **b** Image of nude mouse tumors derived from HK1 cells stably transfected with *RERG* or empty vector. Arrows indicate positions and locations of tumors. **c** The average weights of tumors in nude mice. **d** Representative photographs of H&E staining, IHC analyses of the expression of RERG and immunofluorescence analyses of the expression of CD34 (red), α-SMA (green) in tumors from nude mice. Nuclei were counterstained by DAPI (blue) in the merged pictures of immunofluorescence analyses. Original magnification is ×200. Bar represents 50 μm. **e** Left, IHC scores of RERG in tumors from nude mice. Middle and right, for immunofluorescence analyses, graphs represent average area fraction (%) ± SD of microvessels/field by CD34 and α-SMA area fraction (%) in tumors from nude mice analyzed by Image J. Data are shown as means ± SD. **: $P < 0.01$, ***: $P < 0.001$ by Mann-Whitney U test or Student's t-test.

Figure 6. RERG suppressed MMPs and pro-angiogenic factors through inhibition of NF-κB signaling. a IHC analyses or immunofluorescence analyses of the expression of NF-κB (p65 and p-p65), IL8, IL6, TIMP-2, MMP-2, and MMP-9 in tumors from nude mice. Nuclei

were counterstained by DAPI (blue) in the merged pictures of immunofluorescence analyses. Original magnification is ×200 inner enlarged magnification is ×400. Bar represents 50 μm and 20 μm, respectively. **b** IHC scores of NF-κB (p65 and p-p65), IL8, IL6, TIMP-2, MMP-2, and MMP-9 in tumors from nude mice. **: $P < 0.01$, ***: $P < 0.001$ by Mann-Whitney U test. **c** Schematic diagram for the molecular basis of *RERG* as a tumor suppressor gene in NPC, based on decreasing cell proliferation and inhibiting migration, invasion and angiogenesis through the ERK/NF-κB signaling pathway.

Table 1. Clinicopathological features of patients.

Clinicopathological features	NPC (n=52)	NNE (n=17)
Age (year) mean ± SD	44.5 ± 13.9	40.1 ± 14.9
Male / Female No. (%)	39/ 13 (75.0/ 25.0)	11/6 (64.7/35.3)
Histological subtype[a] No. (%)		
Keratinizing squamous cell carcinoma	1 (1.9)	
Non-keratinizing carcinoma	51(98.1)	
TNM classification[b] No. [c] (%)		
Tumor size No. (%)		
T1	10 (23.3)	
T2	13 (30.2)	
T3	14 (32.6)	
T4	6 (13.9)	
Lymph node metastasis No. (%)		
N0	12 (27.9)	
N1	12 (27.9)	
N2	7 (16.2)	
N3	12 (27.9)	
Metastasis No. (%)		
M0	43 (100)	
M1	0 (0)	
Cancer stage[b] No. [c] (%)		
I- II	13 (30.2)	
III- IV	30 (69.8)	

a: according to the WHO histological classification of tumors of the nasopharynx.

b: according to the International Union Against Cancer (UICC).

c: missing of 9 patient data because of no follow-up.

Fig. 1

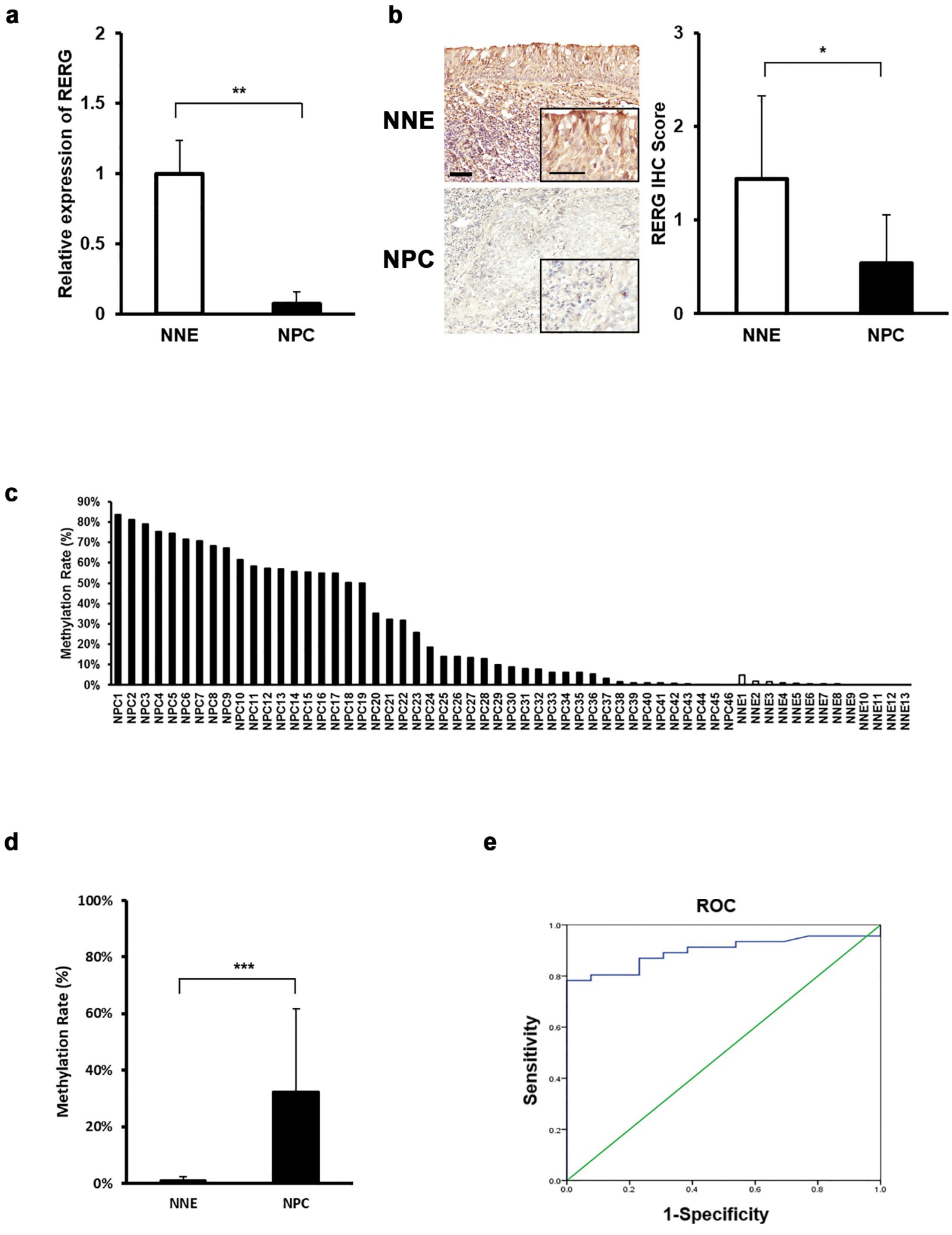
a
Relative expression of RERG
2
1.5
1
0.5
0
**
NNE
NPC
b
NNE
NPC
RERG IHC Score
3
2
1
0
*
NNE
NPC
c
Methylation Rate (%)
90%
80%
70%
60%
50%
40%
30%
20%
10%
0%
NPC1 NPC2 NPC3 NPC4 NPC5 NPC6 NPC7 NPC8 NPC9 NPC10 NPC11 NPC12 NPC13 NPC14 NPC15 NPC16 NPC17 NPC18 NPC19 NPC20 NPC21 NPC22 NPC23 NPC24 NPC25 NPC26 NPC27 NPC28 NPC29 NPC30 NPC31 NPC32 NPC33 NPC34 NPC35 NPC36 NPC37 NPC38 NPC39 NPC40 NPC41 NPC42 NPC43 NPC44 NPC45 NPC46 NNE1 NNE2 NNE3 NNE4 NNE5 NNE6 NNE7 NNE8 NNE9 NNE10 NNE11 NNE12 NNE13
d
Methylation Rate (%)
100%
80%
60%
40%
20%
0%
***
NNE
NPC
e
ROC
Sensitivity
1.0
0.8
0.6
0.4
0.2
0.0
0.0
0.2
0.4
0.6
0.8
1.0
1-Specificity

Fig. 2

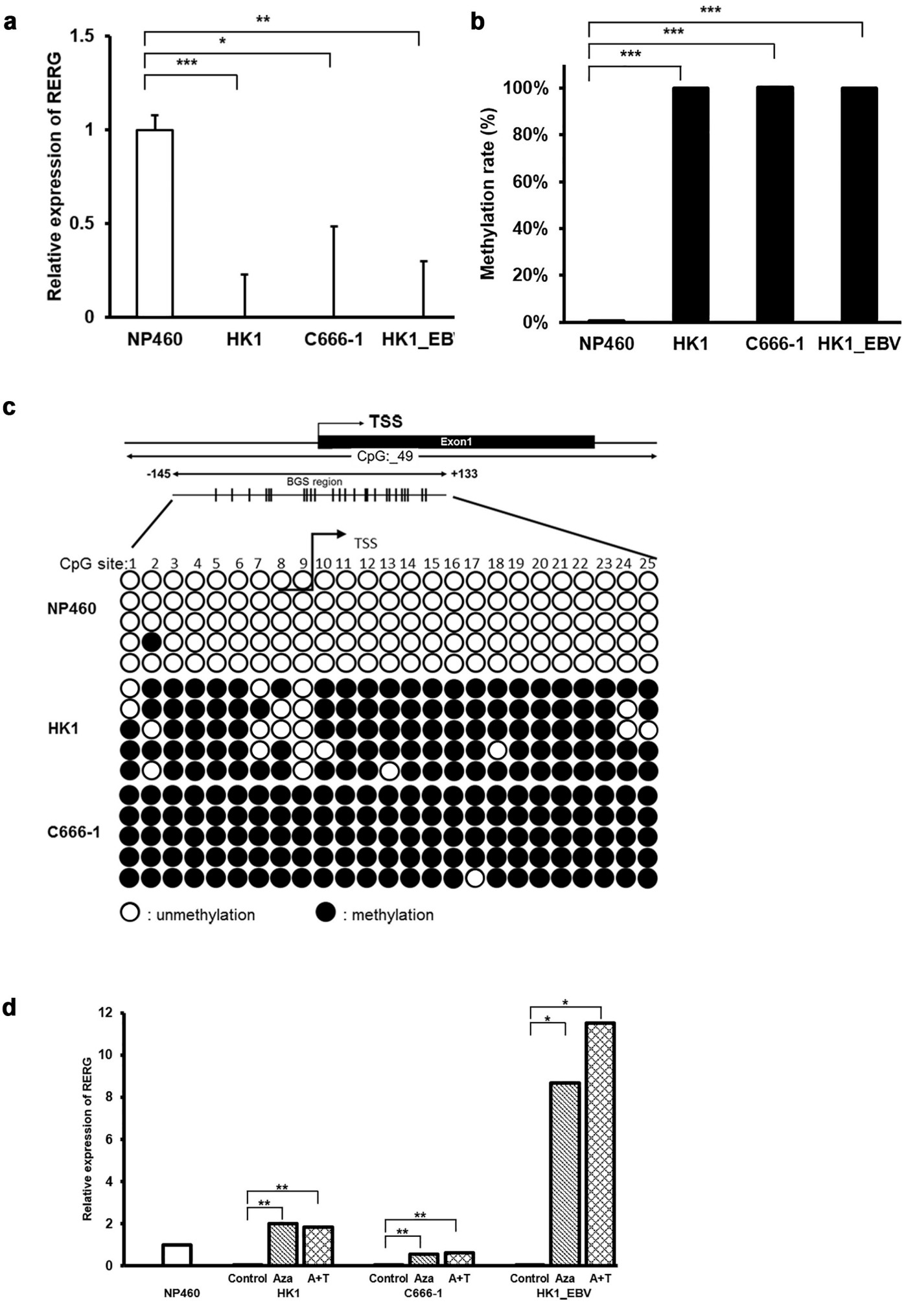
a
Relative expression of RERG
1.5
1
0.5
0
**
*
***
NP460
HK1
C666-1
HK1_EB
b
Methylation rate (%)
100%
80%
60%
40%
20%
0%
***
***
***
NP460
HK1
C666-1
HK1_EBV
c
TSS
Exon1
CpG:_49
-145
+133
BGS region
TSS
CpG site:1 2 3 4 5 6 7 8 9 10 11 12 13 14 15 16 17 18 19 20 21 22 23 24 25
NP460
HK1
C666-1
: unmethylation
: methylation
d
Relative expression of RERG
12
10
8
6
4
2
0
**
**
**
**
*
*
Control Aza A+T
NP460
Control Aza A+T
HK1
Control Aza A+T
C666-1
Control Aza A+T
HK1_EBV

Fig. 3

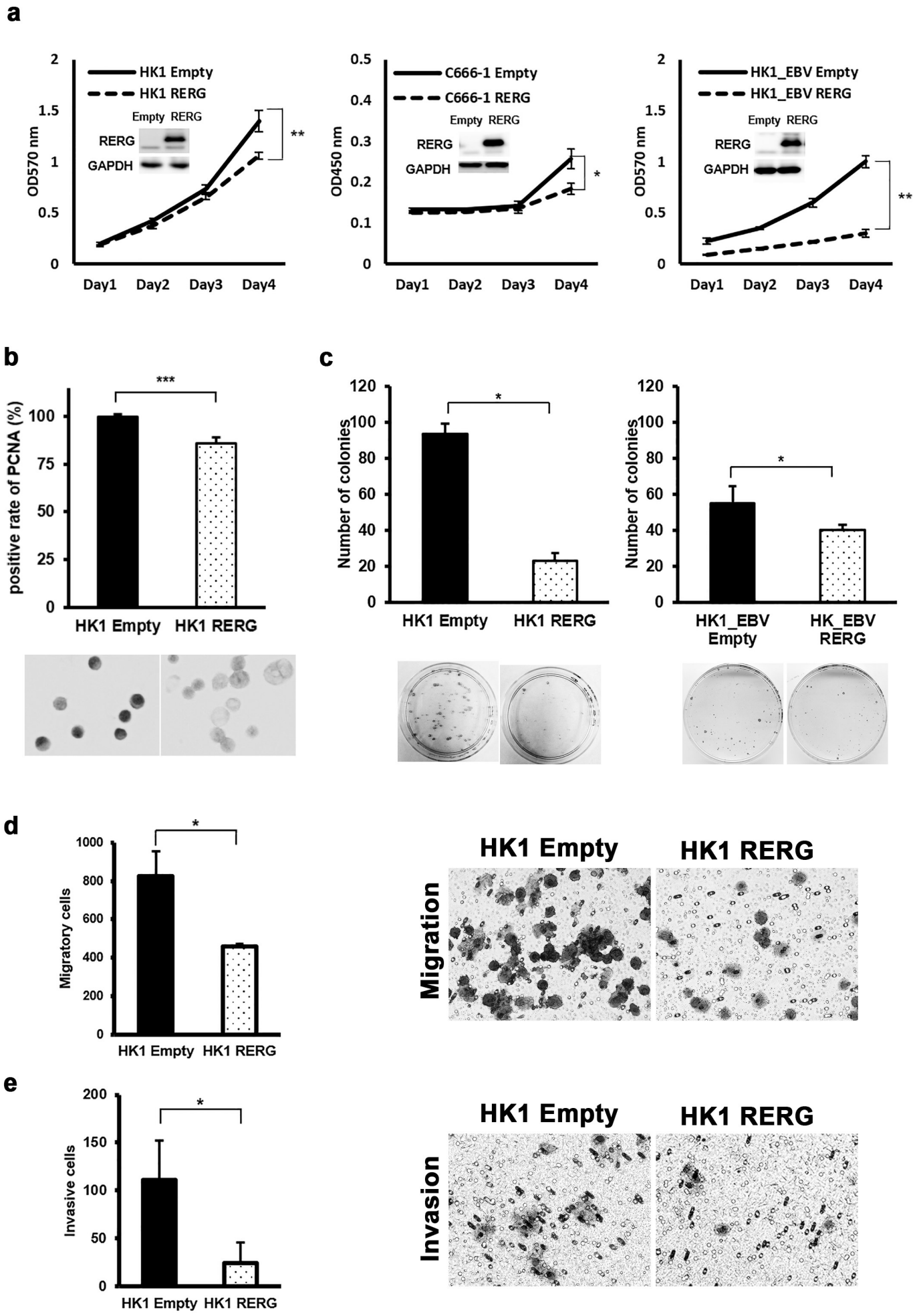
a
HK1 Empty
HK1 RERG
OD570 nm
Empty RERG
RERG
GAPDH
Day1 Day2 Day3 Day4
C666-1 Empty
C666-1 RERG
OD450 nm
HK1_EBV Empty
HK1_EBV RERG
b
positive rate of PCNA (%)
HK1 Empty HK1 RERG
c
Number of colonies
HK1_EBV Empty
HK_EBV RERG
d
Migratory cells
Migration
e
Invasive cells
Invasion

Fig. 4

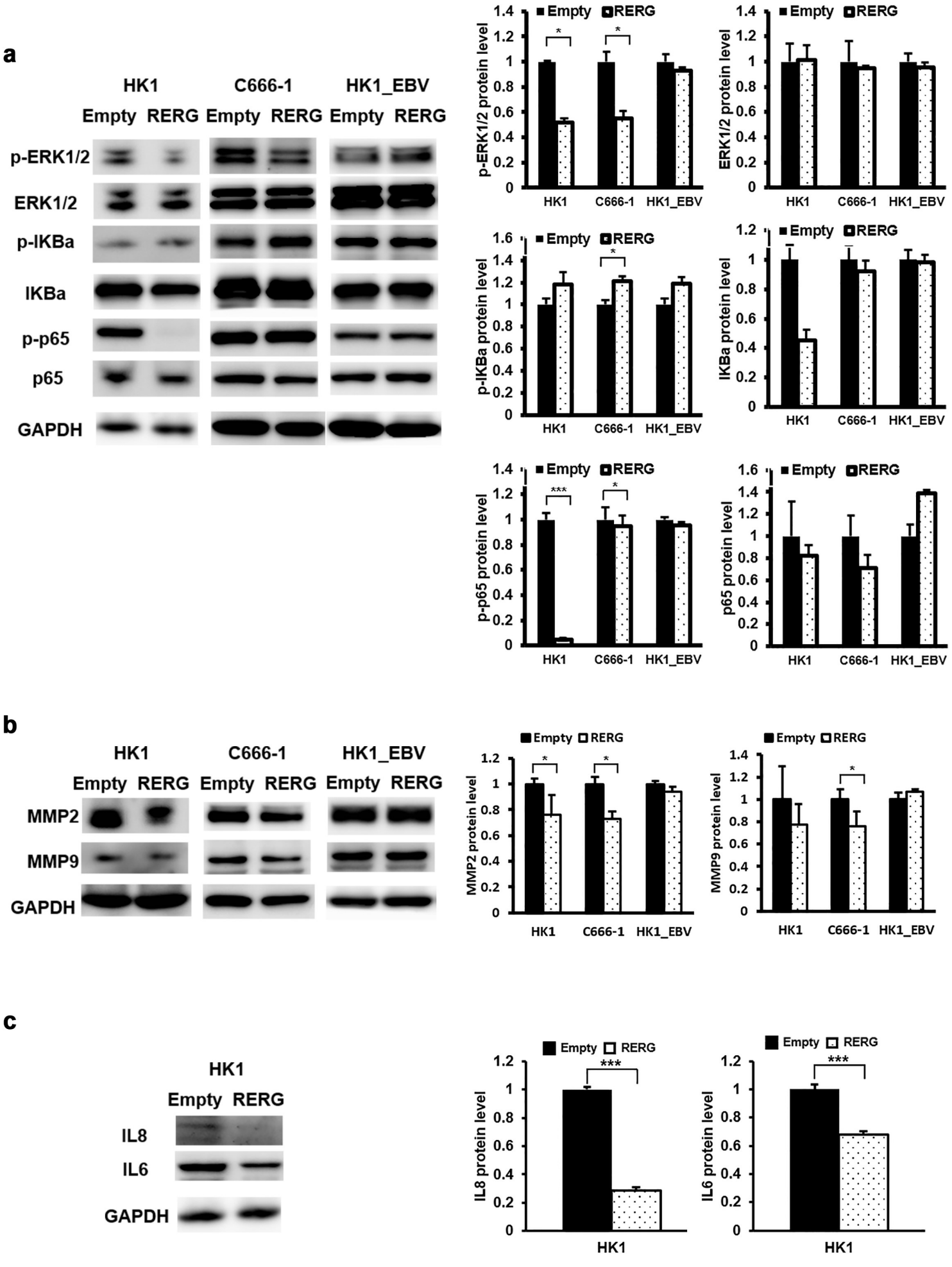
a
HK1
C666-1
HK1_EBV
Empty
RERG
p-ERK1/2
ERK1/2
p-IKBa
IKBa
p-p65
p65
GAPDH
p-ERK1/2 protein level
ERK1/2 protein level
p-IKBa protein level
IKBa protein level
p-p65 protein level
p65 protein level
b
MMP2
MMP9
MMP2 protein level
MMP9 protein level
c
IL8
IL6
IL8 protein level
IL6 protein level

Fig. 5

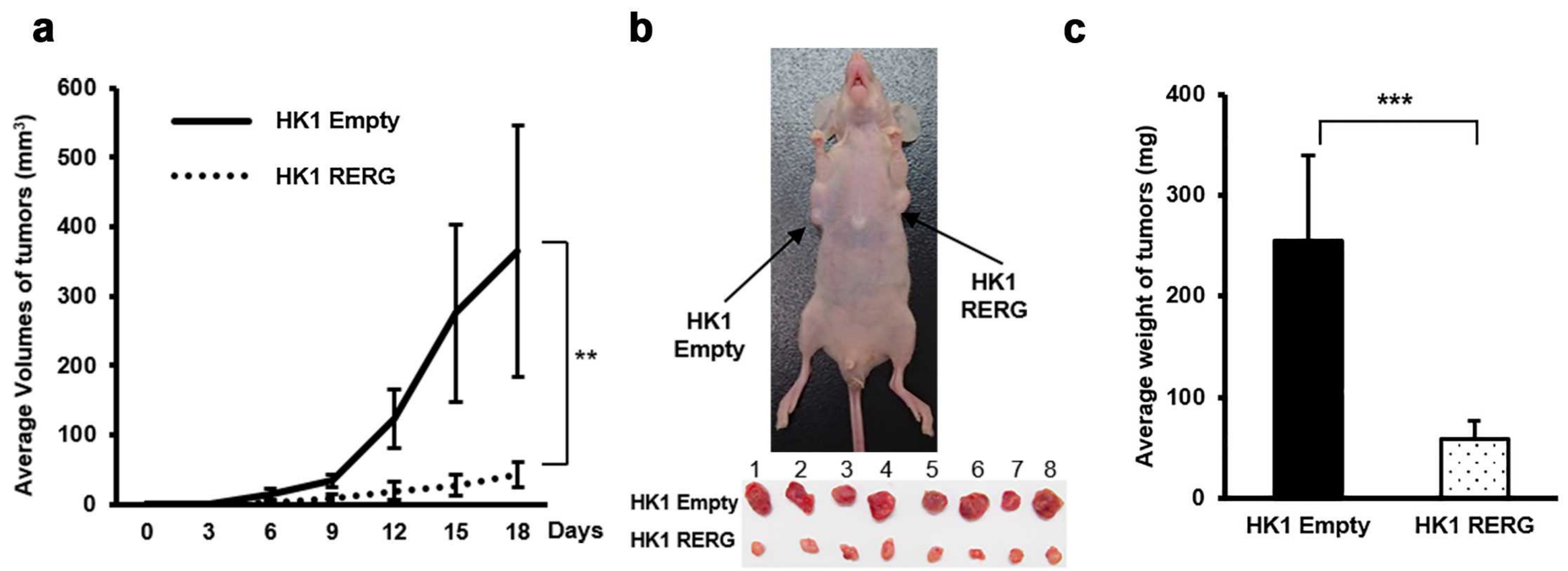
a
Average Volumes of tumors (mm3)
HK1 Empty
HK1 RERG
**
Days
b
HK1 Empty
HK1 RERG
1 2 3 4 5 6 7 8
c
Average weight of tumors (mg)
***
HK1 Empty
HK1 RERG
d
H & E
RERG
CD34
α-SMA
HK1 Empty
HK1 RERG
e
RERG IHC Score
**
CD34 area fraction (%)
***
α-SMA area fraction (%)
**
HK1 Empty
HK1 RERG

Fig. 6

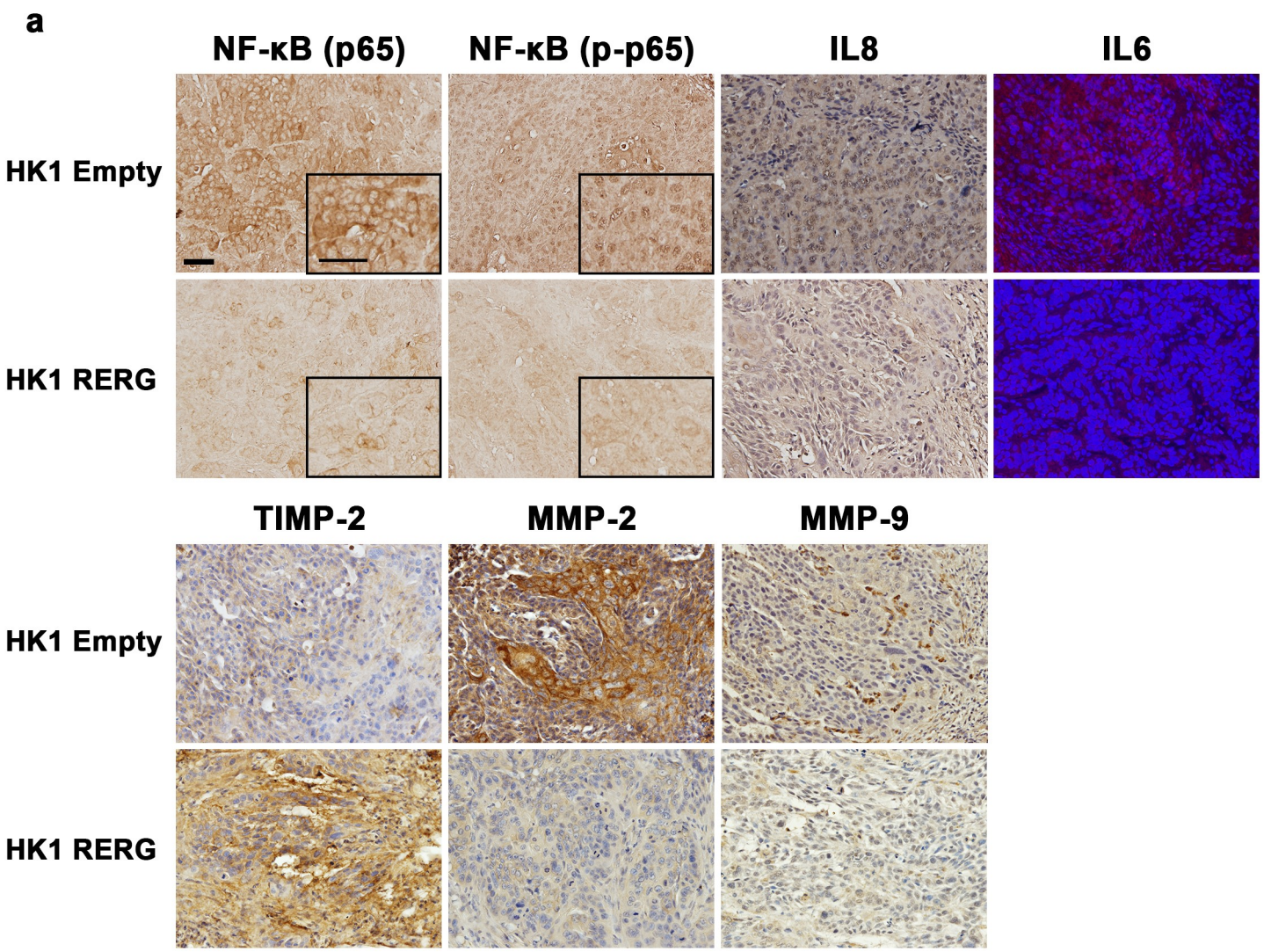
a
NF-κB (p65)
NF-κB (p-p65)
IL8
IL6
HK1 Empty
HK1 RERG
TIMP-2
MMP-2
MMP-9
HK1 Empty
HK1 RERG

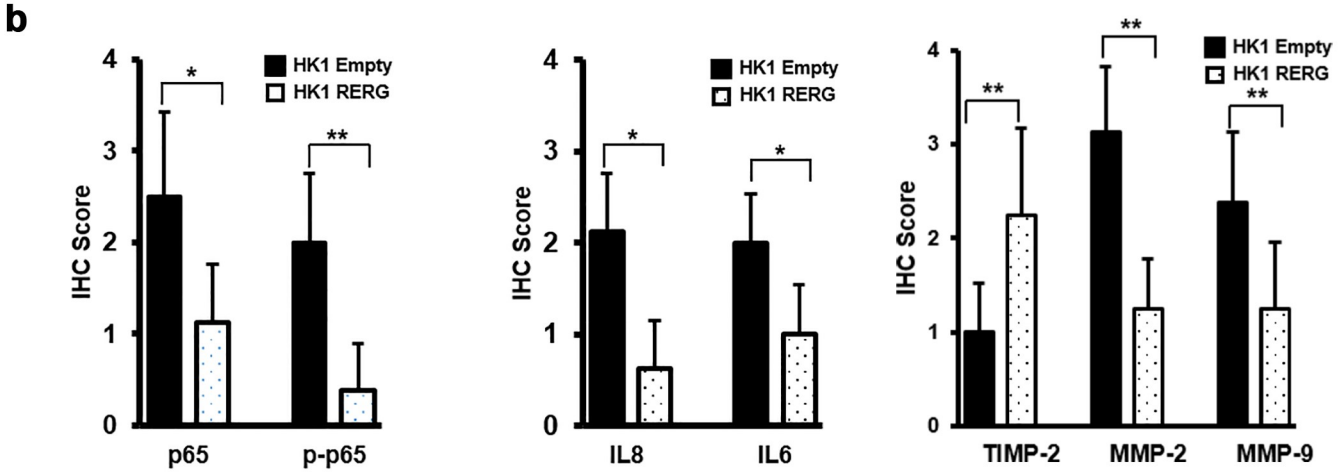
b
IHC Score
HK1 Empty
HK1 RERG
p65
p-p65
IL8
IL6
TIMP-2
MMP-2
MMP-9

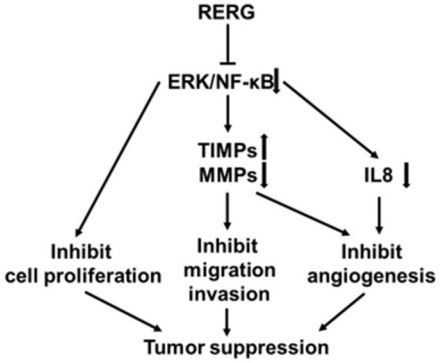
c
RERG
ERK/NF-κB
TIMPs
MMPs
IL8
Inhibit cell proliferation
Inhibit migration invasion
Inhibit angiogenesis
Tumor suppression

Table S1. List of primary antibodies used in the study.

Antibody name	Source	Catalog No.	Host	Dilution	Size (kDa)	Note
RERG	Proteintech	10687-1-AP	Rabbit	1:2000	23	WB
MMP-2	Cell Signaling Technology Inc.	4022	Rabbit	1:1000	72	WB
MMP-9	Santa Cruz Biotechnology Inc.	sc-6840	Goat	1:200	92	WB/IHC
p44/42 MAPK (ERK1/2)	Cell Signaling Technology Inc.	4695	Rabbit	1:1000	42, 44	WB
Phospho-p44/42 MAPK (ERK1/2) (Thr202/Tyr204)	Cell Signaling Technology Inc.	4370	Rabbit	1:1000	44, 42	WB
p65	Cell Signaling Technology Inc.	8242	Rabbit	1:1000	65	WB/IHC
Phospho-p65 (Ser536)	Cell Signaling Technology Inc.	3033	Rabbit	1:1000	65	WB/IHC
IkBα	Cell Signaling Technology Inc.	4814	Mouse	1:1000	39	WB
Phospho-IkBα(Ser32/36)	Cell Signaling Technology Inc.	9246	Mouse	1:1000	40	WB
GAPDH	Abcam	ab9485	Rabbit	1:2500	40	WB
RERG	Sigma-Aldrich	HPA041387	Rabbit	1:200		IHC
TIMP-2	Santa Cruz Biotechnology Inc.	sc-5539	Rabbit	1:200		IHC
MMP-2	Kyowa Pharma Chemical Inc.	F-73	Mouse	1:200		IHC
PCNA	Novocastra Leica	NCL-L-PCNA	Mouse	1:100		ICC/IHC
p65	Santa Cruz Biotechnology Inc.	sc-8008	Mouse	1:200		IHC
CD34	Monosan	MON-RTU1042	Mouse	1:200		IHC
α-SMA	Abcam	ab5694	Rabbit	1:200		IHC
VEGF	Abcam	ab46154	Rabbit	1:1000	43	WB/IHC
IL8	Abcam	ab7747	Rabbit	1:100	11.1	WB/IHC
IL6	Abcam	ab6672	Rabbit	1:1000	25, 50	WB/IF

Supplement method

Methyl-capture sequencing

Genomic DNA from 7 NPC biopsies and 5 NNE samples were extracted using a QIAamp DNA Mini Kit (Qiagen). DNA was fragmented to obtain the desired length of 150 bp by an ultra-sonicator (Covaris, Woburn, MA). We employed the MethylMiner Methylated DNA Enrichment Kit (Invitrogen) to select methylated DNA from 12.5 μg DNA fragments. The final two fractions of highly methylated DNA, which corresponded to gradient elution buffer concentrations of 0.6 M and 2 M NaCl, were collected. The recovered DNA in the 2 M NaCl elution buffer was purified with a PureLink PCR Purification Kit (Invitrogen). After purification, DNA samples were prepared, subjected to PCR and followed by SOLiD sequencing, that were performed by Mie University Life Science Research Center using a SOLiD System (Applied Biosystems, Foster City, CA) with mapping to the human reference genome (hg 19). Sequence data was processed using Partek Genomics Suite (Partek Incorporated, Saint Louis, MO) for further statistical analyses.

Gene expression array analysis

The same tissue samples as for methyl-capture sequencing were used to extract RNA by using mirVana miRNA Isolation Kit (Ambion, Carlsbad, CA, USA) according to the

manufacturer's instructions. Fifty nanograms of RNA were subjected to Agilent SurePrint G3 Human GE microarray analysis (8 x 60K, 1 color, Agilent Technologies, Santa Clara, CA) for gene expression evaluation (Hokkaido System Science, Sapporo, Japan).

Supplement figure legend

Figure S1. Analysis of RAS type GTPase family genes in nasopharyngeal carcinoma primary tumors and nasopharyngeal epithelial tissues.

(A, B) Heat map of RAS type GTPase family in NPC (n=7) and NNE (n=5) tissues. (A) RAS type GTPase family genes expression alerted using cDNA microarray. (B) Hypermethylated genes of RAS type GTPase family by methylated-DNA capture sequencing. (C) Genes of RAS type GTPase family which were significantly downregulated in cDNA microarray and hypermethylated in methylated-DNA capture sequencing.

Figure S2. Analysis of VEGF and SASP factors *in vitro* and *in vivo*.

(A) VEGF in *RERG*-transfected and empty-vector-transfected NPC cells (HK1, C666-1) were determined by western blotting (n=3). (B) mRNA expression of *RERG*, *IL8*, *IL1β* and *TNFα* in xenografts of nude mice was determined by qRT-PCR (n=8). *GAPDH* was used as an internal control. (C) IHC analyses of the expression of VEGF in tumors from nude mice. Original magnification is ×200. Bar represents 50 μm. Data are shown as means ± SD. **: $P < 0.01$, ***: $P < 0.001$ by Student's t-test or Mann-Whitney U test.

Additional file

Fig. S1

A

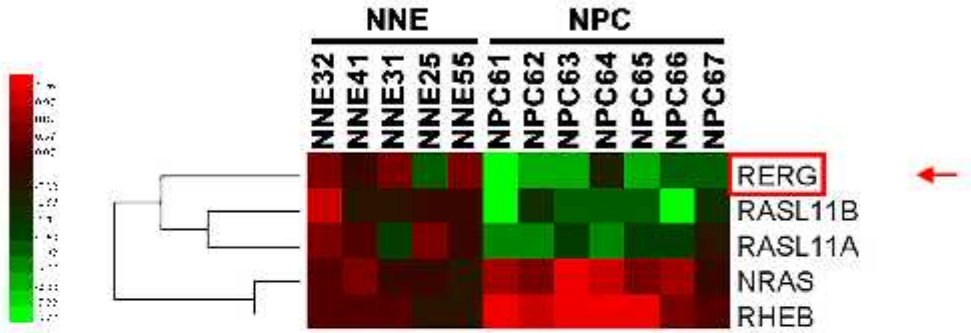

B

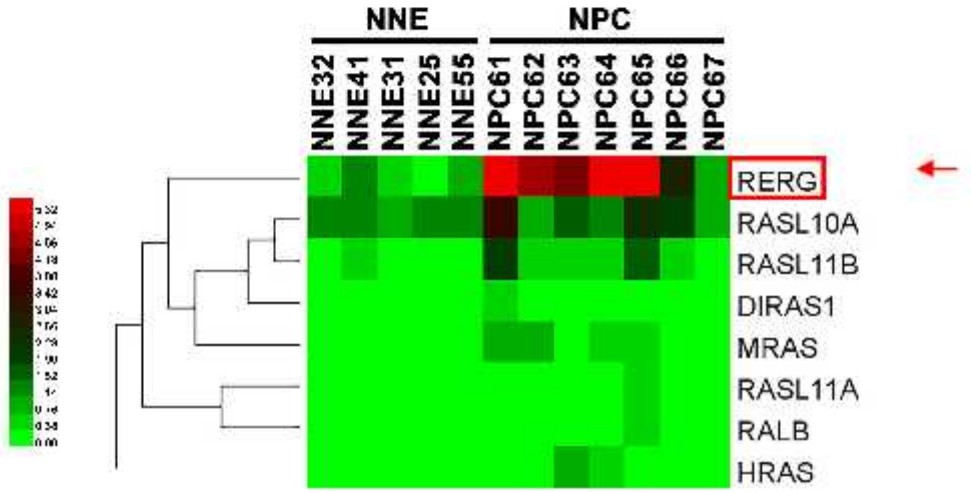

C

Gene symbol	Gene expression fold change (log2)	DNA methylation in RPKM NPC/NNE (fold change)		Description
RERG	-1.90	4.20/0.81	(5.22)	RAS-like, estrogen-regulated, growth inhibitor
RASL11A	-1.44	0.16/0.00	(∞)	RAS-like, family 11, member A
RASL11B	-1.78	0.91/0.27	(3.31)	RAS-like, family 11, member B

Additional file

Fig. S2